Available online at www.sciencedirect.com
ScienceDirect
Trans. Nonferrous Met. Soc. China 23(2013) 1882−1889
Transactions of Nonferrous Metals Society of China
www.tnmsc.cn

Effect of minor Zr and Sc on microstructures and mechanical properties of Al−Mg−Si−Cu−Cr−V alloys

Yi MENG, Zhi-hao ZHAO, Jian-zhong CUI

Key Laboratory of Electromagnetic Processing of Materials of Ministry of Education, Northeastern University, Shenyang 110819, China

Received 11 June 2012; accepted 14 May 2013

Abstract: The effects of minor contents of Zr and Sc on the microstructures and mechanical properties of Al−Mg−Si−Cu−Cr−V alloy were studied. The results show that the effects of minor Zr and Sc on the as-cast grain refinement in the ingots, the improvement in the strength of the as-extruded alloys and the restriction of high angle grain boundaries in the aged alloys can be sorted as Al_3Sc>$Al_3(Zr,Sc)$>Al_3Zr. None of them could stop the nucleation of recrystallization, but $Al_3(Zr,Sc)$ phase is a more effective inhibitor of dislocation movement compared to Al_3Sc in the aged alloys. Compared with the mechanical properties of the aged alloy added only 0.15% Sc, the joint addition of Zr and Sc to the alloy leads to a very slight decrease in strength with even no cost of ductility. Taking both the production cost and the little bad influence on mechanical properties into consideration, an optimal content of Zr and Sc in the Al−Mg−Si−Cu−Cr−V alloy to substitute 0.15% Sc is 0.13% Zr+0.03% Sc.

Key words: Al−Mg−Si−Cu alloy; recrystallization; microstructure; mechanical property

1 Introduction

6xxx aluminum alloys whose main strengthening phases are Mg_2Si are widely used in automotive and construction industries due to the excellent plasticity, favorable corrosion resistance, good weld ability and low scrap compatibility [1−3]. A new Al−Mg−Si−Cu−Cr−V alloy has been investigated, both its ingot-T6 and extrusion-T6 treated alloys have high strength and good plasticity [4,5]. However, based on previous works, complete recrystallization is present in the alloy after hot extrusion or the subsequent solid solution treatment.

It is well known [6] that most of the transition elements increase the recrystallization temperature of the aluminum alloys. The influence degrees on the increase of the recrystallization temperatures are Zr>Ti>Mo>Nb>Cr>Mn>V. Additionally, the rare earth element Sc also belongs to the transition element, and the effect of Sc on the increase of recrystallization temperature is larger than that of any other rare earth elements and transition elements in the aluminum alloys. With the help of Sc addition, the recrystallization temperatures of the aluminum alloys are even higher than their solidus temperatures. So Sc can be considered the optimal anti-recrystallization element in the aluminum alloys. However, due to the high price of Sc element and its few reserves in the earth, its applications in the aluminum alloys are limited. In order to decrease the cost of aluminum alloys, Zr is used to substitute Sc partially. When both Zr and Sc are added to the aluminum alloys, the eutectic composition of Al−Al_3Sc is reduced, and the $Al_3Sc_{1-x}Zr_x$ particles are formed by means of the substitution of Sc for Zr. The $Al_3Sc_{1-x}Zr_x$ particles have all of the favorable characteristics of Al_3Sc particles and higher thermal stability [7,8]. Many literatures [9−11] reported the effects of minor Zr and Sc on the microstructures and mechanical properties of Al−Mg alloys and Al−Zn−Mg−Cu alloys, but few researches investigated those on the Al−Mg−Si−Cu alloys.

In this study, the effects of minor Zr and Sc on the microstructures and mechanical properties of the Al−Mg−Si−Cu−Cr−V alloy were investigated. An optimal content of Zr and Sc in the Al−Mg−Si−Cu−Cr−V alloy was obtained to improve the strength with little cost of ductility. Both the existence forms and strengthening mechanisms were discussed. As a result, a low cost Al−Mg−Si−Cu−Cr−V alloy with unique joint

Foundation item: Projects (N110609002, N110408005) supported by the Fundamental Research Funds for Northeastern University, China
Corresponding author: Jian-zhong CUI; Tel: +86-24-83671738; E-mail: yimonmy@sina.com; jzcui@epm.neu.edu.cn
DOI: 10.1016/S1003-6326(13)62673-4

addition of Zr and Sc was identified.

2 Experimental

The nominal compositions of the alloys used in this study were listed in Table 1. Si, Sc and V were introduced by means of Al−23Si, Al−2Sc and Al−4V (mass fraction, %) master alloys, respectively, Cr and Zr were put into the alloy in the form of chromium tablet and zirconium tablet (contain 63% Cr and 85% Zr respectively including burning loss). Other elements were introduced by relevant commercial pure metals. The contents of (Zr+Sc) added in each alloy are almost the same (about 0.15%−0.16%) to eliminate the effect of different amounts of (Zr+Sc) on the microstructures and mechanical properties of the new Al−Mg−Si−Cu alloy. The alloy was melted in a graphite crucible inside a medium frequency induction furnace. Ingots with diameter of 60 mm were prepared with water-cooling copper mold at 750 °C after the melt was degassed, slag removed and refined. Then they were machined into ingots with dimensions of *d*46 mm×90 mm after homogenization for hot extrusion. At last, the bars with diameter of 12 mm were produced at 430 °C by means of backward extrusion. The heat treatment and hot extrusion process were illustrated in Fig. 1. The mechanical tests for as-extruded alloys and aged alloys were conducted at room temperature. At least three tensile samples for each case were tested by CMT5105 universal test machine to obtain the mechanical properties at a constant ram velocity of 2 mm/min. The microstructures were observed by optical microscope, scanning electron microscope (SEM), transmission electron microscope (TEM) with energy dispersive X-ray spectrometer (EDS).

Table 1 Chemical composition of text alloys

Alloy	Compositional/%								Ratio of Zr to Sc
	Mg	Si	Cu	Cr	V	Ti	Zr	Sc	
A	1.37	1.15	0.82	0.12	0.15	0.03	0	0	0
B	1.37	1.15	0.82	0.12	0.15	0.03	0.15	0	−
C	1.37	1.15	0.82	0.12	0.15	0.03	0.13	0.03	4:1
D	1.37	1.15	0.82	0.12	0.15	0.03	0.10	0.05	2:1
E	1.37	1.15	0.82	0.12	0.15	0.03	0.05	0.1	1:2
F	1.37	1.15	0.82	0.12	0.15	0.03	0	0.15	0

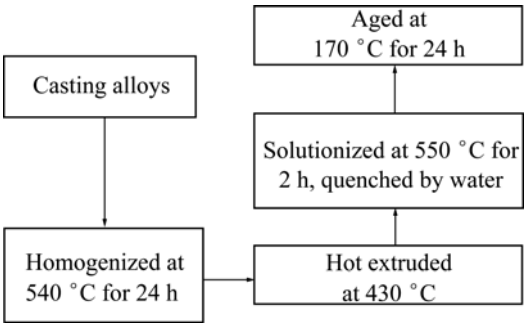

Fig. 1 Heat treatment and extrusion process for alloys

3 Results and discussion

3.1 Effects of Zr and Sc on microstructure of ingots

Figure 2 shows the as-cast microstructures of the Al−Mg−Si−Cu−Cr−V alloys with different additions of Zr and Sc elements. Figure 2(a) indicates that the as-cast microstructure of the base alloy is characterized by coarse dendritic grains. Figure 2(b) illustrates that the as-cast grains are refined to some extent when the alloy is added only 0.15% Zr. Both the as-cast grain sizes of alloys C and D are similar to that of alloy B, as shown in Figs. 2(c) and (d). Figure 2(e) shows that a further reduction in the as-cast grain size is carried out in alloy E. While the finest as-cast grains are present in the microstructure of the alloy with only 0.15% Sc addition as shown in Fig. 2(f), almost all of them become into equiaxed grains. It means that both Zr and Sc have the ability to refine the as-cast grains, and the effect of Sc on the as-cast grain refinement is much larger than that of Zr. The as-cast grain size of the alloy decreases with the increase of Sc content. The joint addition of Zr and Sc leads to the formation of $Al_3(Zr, Sc)$ particles. When the ratio of Zr to Sc is 4:1 or 2:1, the slight difference of Zr content and the small amounts of $Al_3(Zr, Sc)$ particles result in the slight grain refinement of the as-cast alloy, compared with alloy B. But when the Sc content reaches up to 0.1%, the Al_3Sc particles lead to an obvious as-cast grain refinement. So the impact of these particles on the as-cast grain refinement of the alloy is Al_3Sc>$Al_3(Zr, Sc)$>Al_3Zr. The reason is that there is a good coherent interface between the fine Al_3Sc particles and α(Al) during solidification, so these Al_3Sc particles promote the non-homogeneous nucleation and as a result, the grains are refined [12]. The $Al_3(Zr,Sc)$ particle has a lower coherency level than the Al_3Sc particle, and Al_3Zr particle has the lowest coherency level among them.

3.2 Effect of Zr and Sc on microstructure of as-extruded alloys

Figure 3 shows the micrographs of the as-extruded alloys in the longitudinal direction. The complete fibrous structures are visible in all of these extrusions due to the short extrusion time, low extrusion temperature and water quench after being extruded. As a result, there is no enough time for the extrusions to carry out the dynamic recrystallization and metadynamic recrystallization, only the as-deformed microstructures are present, as shown in Fig. 3.

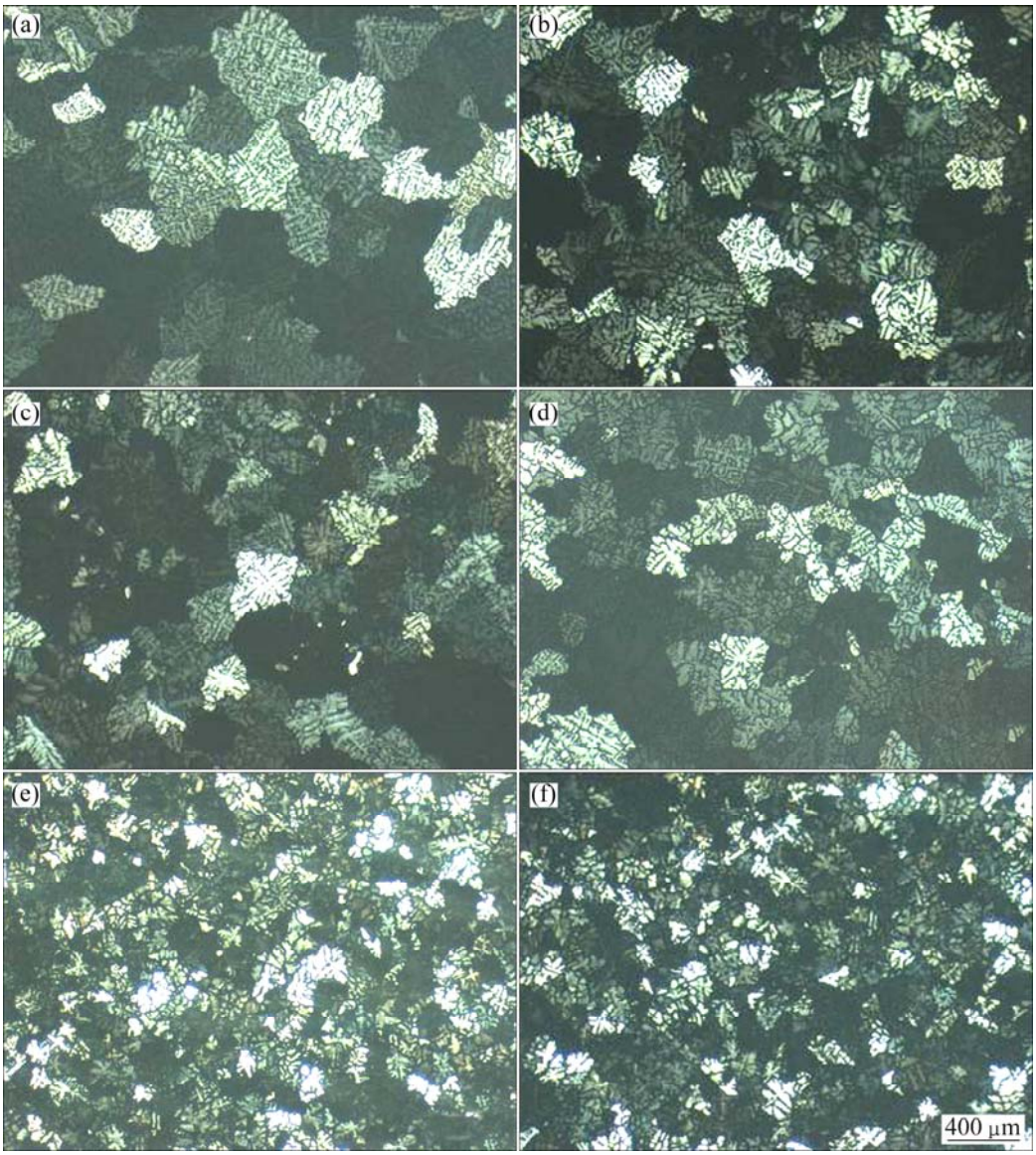

Fig. 2 OM images of as-cast alloys: (a) Alloy A; (b) Alloy B; (c) Alloy C; (d) Alloy D; (e) Alloy E; (f) Alloy F

Figure 4 shows the SEM image of the as-extruded alloy C in the longitudinal direction. The distribution of Zr in the as-extruded microstructure shown in Fig. 4(a) is illustrated in Fig. 4(b). It is obvious that some Zr containing phases with elliptical shape exist in the alloy. The EDS analysis results are shown in Figs. 4(c) and (d). Figure 4(c) indicates that Zr exists in the as-extruded alloy in the form of Al_3Zr particles with elliptical morphology, and Fig. 4(d) shows that some Zr atoms are substituted by Sc atoms to form elliptical $Al_3(Zr,Sc)$ phases.

3.3 Effect of Zr and Sc on microstructure of aged alloys

Figure 5 shows the micrographs of the aged alloys in longitudinal direction. The static recrystallization is visible in all the aged alloys. It is indicated that none of the Al_3Zr particles, Al_3Sc particles and $Al_3(Zr,Sc)$ particles can stop the nucleation of recrystallization in the aged alloys, but some of these particles can inhibit the growth of recrystallization by hindering the migration of grain boundaries to a certain degree. Figure 5(a) shows that the recrystallized grains of aged alloy A with long belt shape grow largest compared with those of other aged alloys B−F. Slight grain refinement in the aged alloy B is observed, as shown in Fig. 5(b), due to the restriction of high angle grain boundaries movement caused by Al_3Zr particles. Further reduction of the recrystallized grain size is visible in the aged alloy C. So it is evident from Fig. 5(c) that the effect of $Al_3(Zr,Sc)$ particles on the recrystallized grain refinement is larger than that of Al_3Zr particles. Based on Figs. 5(d)−(f), the grain size reduces with the increase of Sc content in the alloys and the finest grains are present in the aged alloy

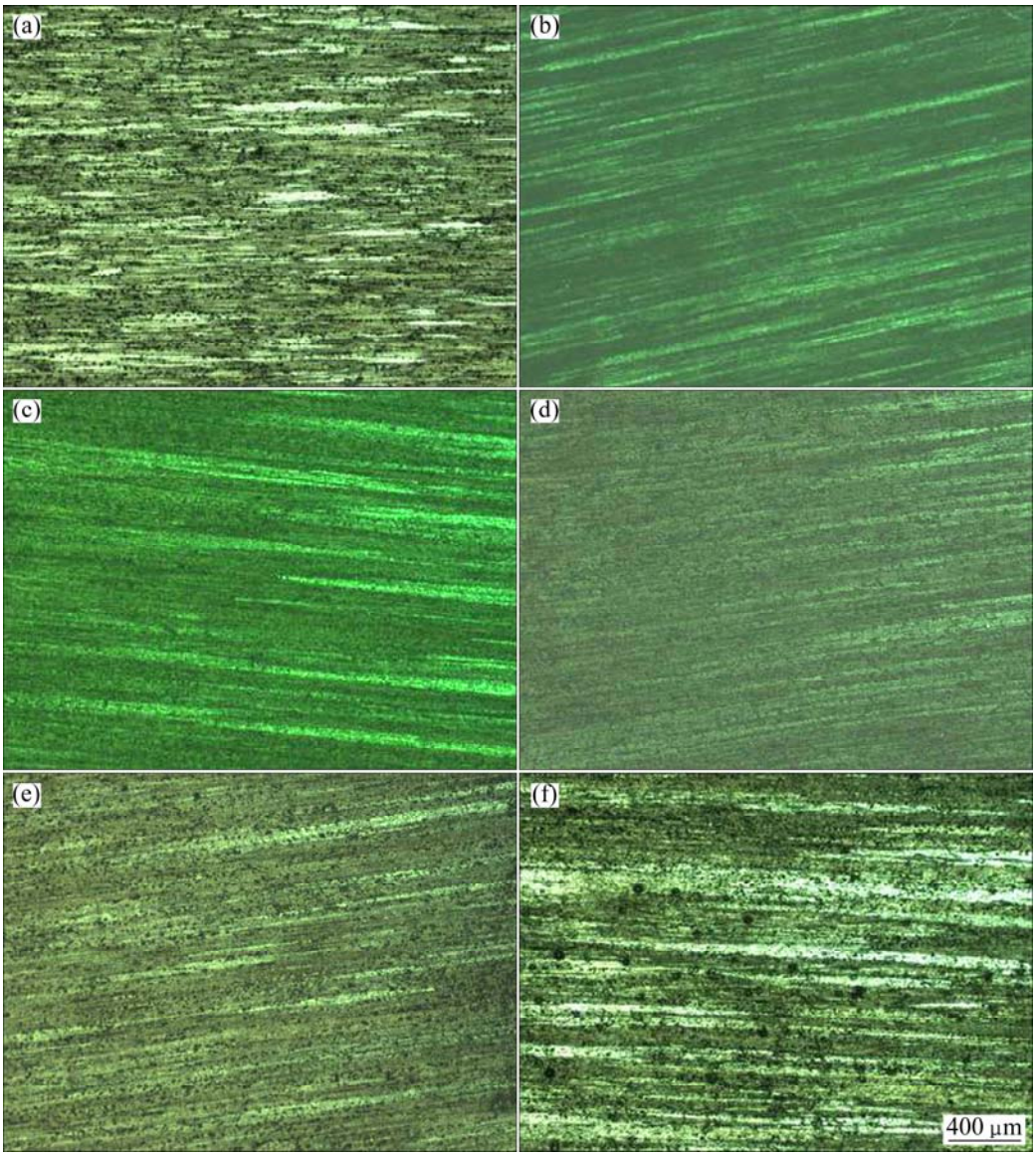

Fig. 3 OM images of as-extruded alloys in longitudinal direction: (a) Alloy A; (b) Alloy B; (c) Alloy C; (d) Alloy D; (e) Alloy E; (f) Alloy F

F. So there is no doubt that Al_3Sc particles have the largest influence on the inhibition of recrystallization. The coherency level of the additions to the aluminum matrix is as below: Al_3Sc>$Al_3(Zr,Sc)$>Al_3Zr.

The TEM micrographs and EDS results of aged alloys B, C and F are shown in Fig. 6 and Table 2, respectively. Figures 6(a) and (c) show that both the Al_3Zr particle and Al_3Sc particle are present with the elliptical morphologies in the aged alloys B and F respectively, while $Al_3(Zr,Sc)$ particle exists in the aged alloy C in the form of spherical shape and its mean diameter is about 48 nm. The characteristics of Al_3Zr, Al_3Sc and $Al_3(Zr,Sc)$ particles to the aluminum matrix are similar to each other [7,13−15]. There is coherent interface between these particles and aluminum solid solution, and these particles which homogenously distribute throughout the matrix can impede the movement of dislocations strongly, make the submicrostructure of extrusions stable, block the sub-boundaries to develop into larger angle grain boundaries, and hinder the formation of grain boundaries and their migration. Although these particles have the similar influence on the microstructures of aged alloys, it can be concluded from Fig. 5 that the effects on the

Table 2 EDS results of phases indicated by arrows in Fig. 6 (molar fraction, %)

Phase	Al	Mg	Si	Cu	V	Cr	Ti	Zr	Sc
C	97.38		0.92	0.69			0.15	0.86	
D	78.89		7.35	1.51				10.90	1.35
E	92.66	3.74	1.01	0.56	1.58	0.28			0.17

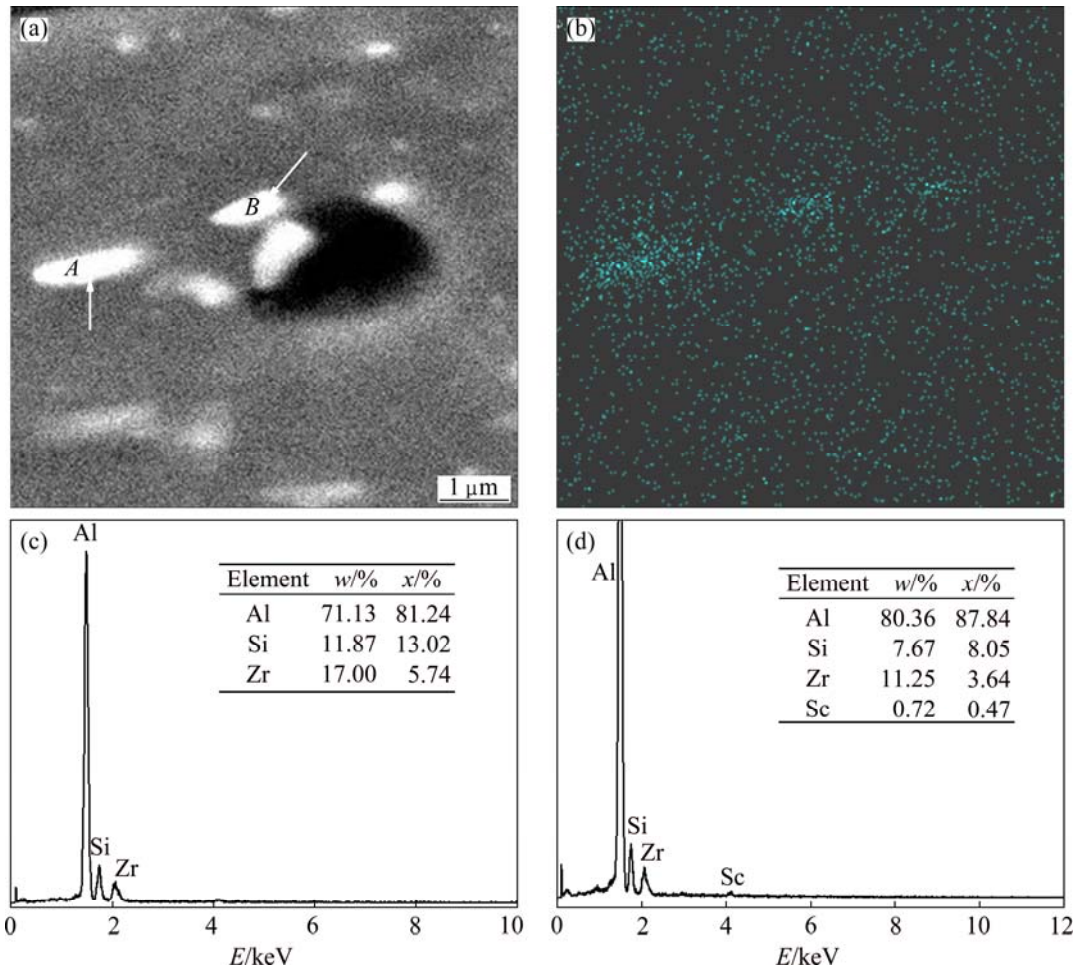

Fig. 4 SEM image and EDS results of as-extruded alloy C in longitudinal direction: (a) SEM image; (b) Distribution of Zr in Fig. 4(a); (c) EDS results of phase *A* indicated by arrow in Fig. 4(a); (d) EDS results of phase *B* indicated by arrow in Fig. 4(a)

restriction of recrystallization behaviors in the aged alloys are quite different. The impacts on inhibiting recrystallization can be ordered as Al_3Sc>Al_3(Zr,Sc)> Al_3Zr.

3.4 Effect of Zr and Sc on mechanical properties of extrusions

Figure 7 illustrates the mechanical properties of the as-extruded alloys and aged alloys, respectively. In Fig. 7 (a), the as-extruded alloy F has the highest strength but the lowest elongation. The ultimate tensile strength is 232 MPa, yield stress is 129 MPa and elongation is 20.65%. The ultimate tensile strength of the as-extruded alloys increases from 213 to 232 MPa with increasing Sc contents, while the elongation decreases from 24.2% to 20.65% with the increase of Sc contents, though the Zr content reduces at the same time. The increasing rate of ultimate tensile strength remains constant at first and increases obviously when the Sc content is more than 0.03% in the as-extruded alloys, but the elongation declines continuously. Based on Fig. 3, the work hardening can not be ignored in all the as-extruded alloys due to the absence of recrystallization. But the reason why different Zr and Sc contents lead to various mechanical properties of as-extruded alloys is that the precipitation-hardening of Al_3Zr, Al_3(Zr, Sc) and Al_3Sc phases are quite different for the as-extruded alloys. Their strengthening effects on the as-extruded alloys are Al_3Sc>Al_3(Zr,Sc)>Al_3Zr, so the reduction of Al_3Zr phases does not result in an obvious decrease in strength but the increase of Al_3(Zr,Sc) and Al_3Sc phases contents would improve the strength of as-extruded alloys significantly.

Figure 7(b) shows the mechanical properties of aged alloys. The aged alloy F still has the highest ultimate tensile strength and yield stress of 432 and 369 MPa respectively with a relatively high elongation of 16%, while those of the aged alloy A are 414 MPa, 355 MPa and 16.1%, respectively. There are likely two reasons, firstly, the dispersion distribution of fine Al_3Sc phases pins the movement of dislocations sharply, and thus enhances shear stress which is needed by dislocation

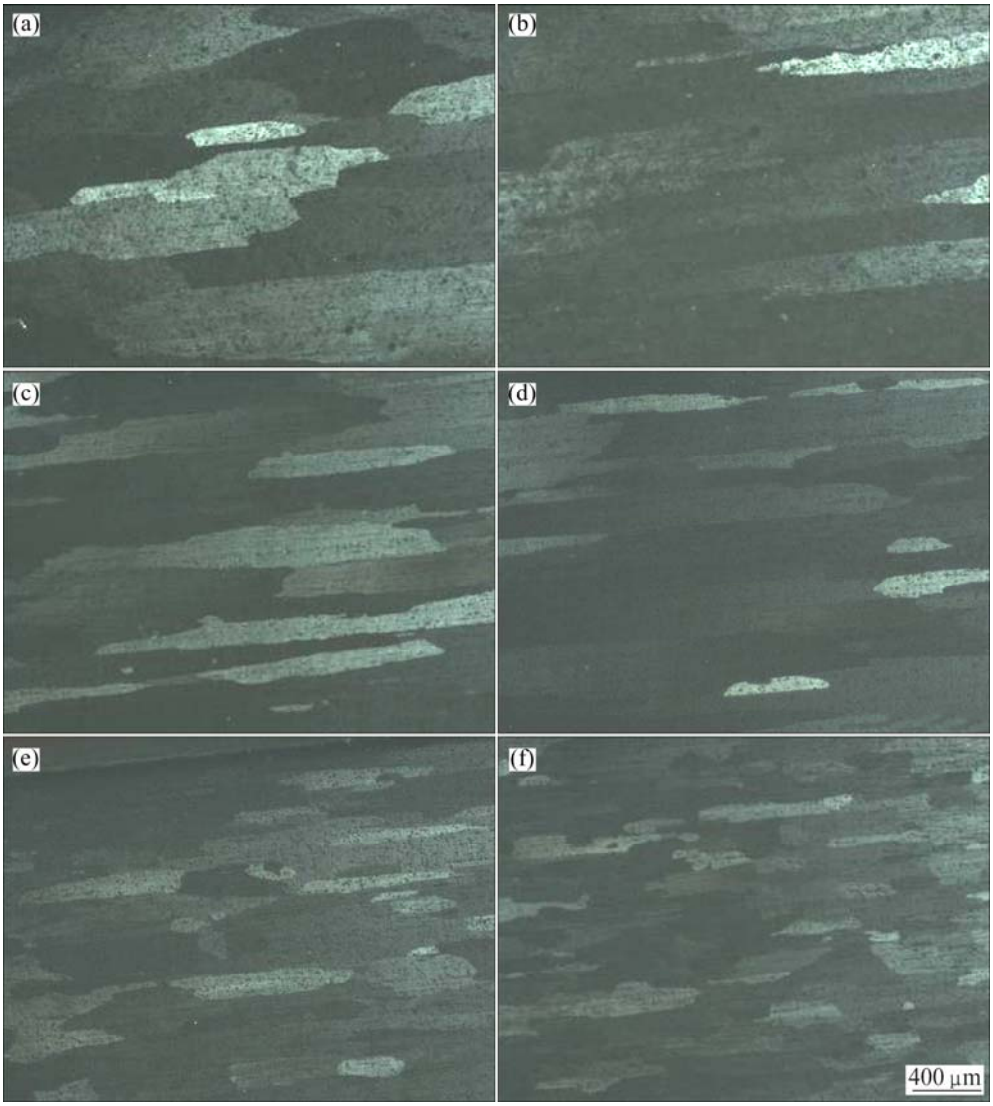

Fig. 5 OM images of aged alloys in longitudinal direction: (a) Alloy A; (b) Alloy B; (c) Alloy C; (d) Alloy D; (e) Alloy E; (f) Alloy F

sliding, and then strengthens the aged alloy [16]. Secondly, Al_3Sc phase aids in the restriction of high angle grain boundaries movement (as shown in Fig. 5) and as a result, the recrystallized grain refinement is visible. Therefore, the addition of 0.15% Sc to the new aged Al−Mg−Si−Cu alloy leads to an improvement in strength compared with aged alloy A, and with no cost of ductility. Although the elongations of aged alloys C (14.6%), D (15.1%) and E (16.2%) are a little different from that of aged alloy F, the strengths are almost the same with each other (range from 429 to 431 MPa). So it can be concluded that the effect of Al_3Sc phase on the improvement of the strength of aged alloys is no more higher than that of $Al_3(Zr,Sc)$ phase. YIN et al [17] reported that the shape of $Al_3(Zr, Sc)$ phase was coffee bean-like in the as-hot deformed aluminum alloy. But in this work, the shape of $Al_3(Zr, Sc)$ phase changes into spherical morphology (as shown in Fig. 6(c)) in the aged alloy C. It is quite different from the elliptical shapes of Al_3Sc phase in the aged alloy F, and thus leads to more efficient inhibition of dislocation movement compared with the Al_3Sc phase. However, Al_3Sc phase has a higher coherency level with aluminum matrix than the $Al_3(Zr,Sc)$ phase. So the complex combination of the shape, coherency level with aluminum matrix and grain refinement result in the similar mechanical properties among alloys C, D, E and F. It is well known that the price of Sc is even higher than that of gold. So it is vital to add Sc into the Al−Mg−Si−Cu−Cr−V alloy as few as possible to reduce its production cost. It is a good way to apply Zr to substitute part of Sc addition into this alloy and with little cost of strength and ductility. Based on the results and discussions above, the proportion of 0.13% Zr and 0.03% Sc is the most acceptable substitution for 0.15% Sc in the alloy due to the lowest production cost and high-enough mechanical properties.

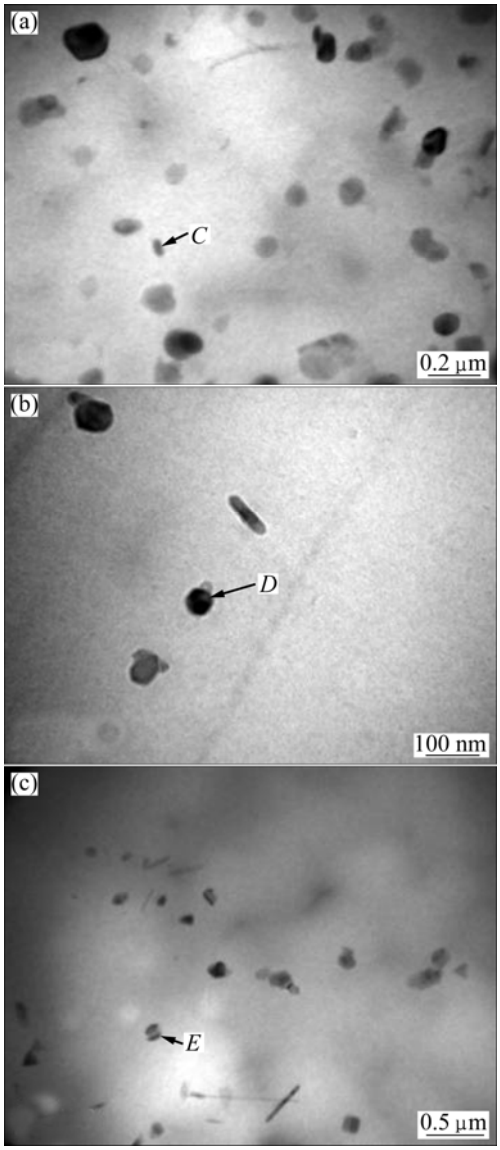

Fig. 6 TEM images of aged alloys: (a) Alloy B; (b) Alloy C; (c) Alloy F

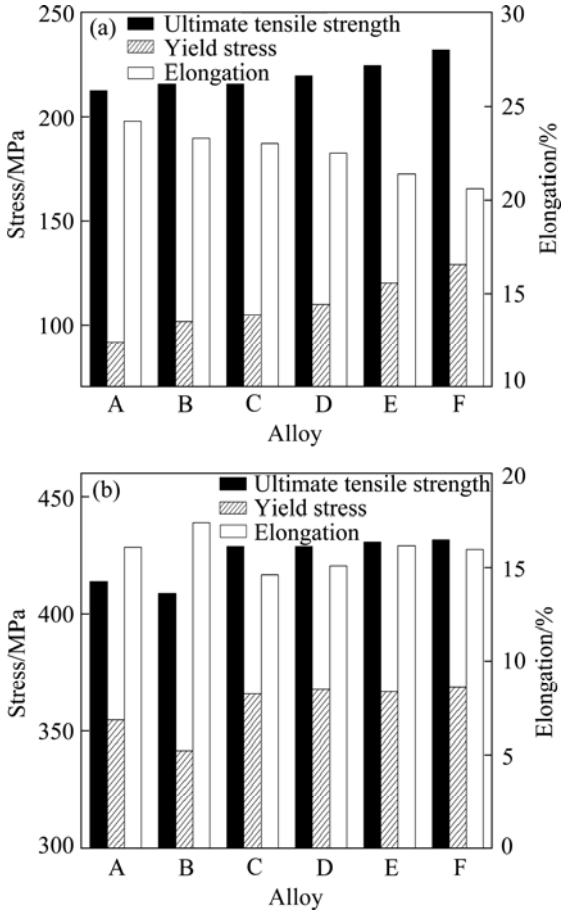

Fig. 7 Tensile properties of as-extruded alloys and aged alloys: (a) As-extruded alloys; (b) Aged alloys

4 Conclusions

1) Both minor Zr and Sc lead to the grain refinement in the as-cast Al−Mg−Si−Cu−Cr−V alloys, and the effects of Zr-containing phases and Sc-containing phases on the as-cast grain refinement are Al_3Sc>$Al_3(Zr,Sc)$>Al_3Zr.

2) The effects of Al_3Zr, Al_3Sc and $Al_3(Zr,Sc)$ phases on the restriction of dislocation movement in the as-extruded Al−Mg−Si−Cu−Cr−V alloys are Al_3Sc> $Al_3(Zr,Sc)$>Al_3Zr.

3) None of the particles including Al_3Zr, Al_3Sc and $Al_3(Zr,Sc)$ phases can restrain the recrystallization for the Al−Mg−Si−Cu−Cr−V extrusions after solid solution treatment, but they can slow down the growth of the recrystallized grains in various degrees. The effect of the inhibition sorted in descending order is proved as Al_3Sc>$Al_3(Zr,Sc)$>Al_3Zr. However, $Al_3(Zr,Sc)$ phases pin the movement of dislocation more efficiently in the aged alloy due to the varying shapes.

4) There is little difference between the mechanical properties of the aged Al−Mg−Si−Cu−Cr−V alloys with the joint addition of 0.15% (Zr+Sc) and the one with only 0.15% Sc addition. Considering the production cost, an optimal content of Zr and Sc in the alloy is 0.13% Zr and 0.03% Sc.

References

[1] ZENG Feng-li, WEI Zhong-ling, LI Jin-feng, LI Chao-xing, TAN Xing, ZHANG Zhao, ZHENG Zi-qiao. Corrosion mechanism associated with Mg_2Si and Si particles in Al−Mg−Si alloys [J]. Transactions of Nonferrous Metals Society of China, 2011, 21(12): 2559−2567.

[2] DINAHARAN I, MURUGAN N. Dry sliding wear behavior of AA6061/ZrB_2 in-situ composite [J]. Transactions of Nonferrous Metals Society of China, 2012, 22(4): 810−818.

[3] RAJAKUMAR S, MURALIDHARAN C, BALASUBRAMANIAN V. Establishing empirical relationships to predict grain size and tensile strength of friction stir welded AA 6061-T6 aluminium alloy joints [J]. Transactions of Nonferrous Metals Society of China, 2010,

20(10): 1863−1872.
[4] BERGSMA S C, KASSNER M E, LI X, WALL M A. Strengthening in the new aluminum alloy AA6069 [J]. Materials Science and Engineering A, 1998, 254(1−2): 112−118.
[5] BERGSMA S C, KASSNER M E, LI X, DELOS-REYES U A, HAYES T A. The optimized mechanical properties of the new aluminum alloy AA6069 [J]. Journal of Materials Engineering and Performance, 1996, 5(1): 111−116.
[6] SU Bei-hua, SHEN Yun-qi. Minor elements of aluminum alloys [J]. Light Alloy Fabrication Technology, 1997, 25(6): 35−37. (in Chinese)
[7] CABIBBO M, EVANGELISTA E. A TEM study of the combined effect of severe plastic deformation and (Zr), (Sc+Zr)-containing dispersoids on an Al−Mg−Si alloy [J]. Journal of Materials Science, 2006, 41(16): 5329−5338.
[8] LITYŃSKA L, ABOU R D, KOSTORZ G, DUTKIEWICZ J. TEM and HREM study of Al_3Zr precipitates in Al−Mg−Si−Zr alloy [J]. Journal of Microscopy, 2006, 223(3): 182−184.
[9] OCENASEK V, SLAMOVA M. Resistance to recrystallization due to Sc and Zr addition to Al−Mg alloys [J]. Materials Characterization, 2001, 47(2): 157−162.
[10] DENG Ying, YIN Zhi-min, ZHAO Kai, DUAN Jia-qi, HE Zhen-bo. Effects of Sc and Zr microalloying additions on the microstructure and mechanical properties of new Al−Zn−Mg alloys [J]. Journal of Alloys and Compounds, 2012, 530: 71−80.
[11] GROBNER J, ROKHLIN L L, DOBATKINA T V, SCHMID-FETZER F R. Predictive calculation of phase formation in Al-rich Al−Zn−Mg−Cu−Sc−Zr alloys using a thermodynamic Mg-alloy database [J]. Journal of Alloys and Compounds, 2007, 433(1−2): 108−113.
[12] TAO Hui-jing, LI Shao-tang, LIU Ji-li, ZHOU Xiang, KANG Ning, YIN Zhi-min. Micro-alloying mechanism of Sc in aluminum alloys [J]. Materials Science and Engineering of Powder Metallurgy, 2008, 13(5): 249−258. (in Chinese)
[13] CAVALIEREA P, CABIBBO M. Effect of Sc and Zr additions on the microstructure and fatigue properties of AA6106 produced by equal-channel-angular-pressing [J]. Materials Characteristic, 2008, 59(3): 197−203.
[14] KENDIG K L, MIRACLE D B. Strengthening mechanisms of an Al−Mg−Sc−Zr alloy [J]. Acta Materialia, 2002, 50(16): 4165−4175.
[15] LI Wen-bin, PAN Qing-lin, XIAO Yan-ping, HE Yun-bin, LIU Xiao-yan. Microstructural evolution of ultra-high strength Al−Zn−Cu−Mg−Zr alloy containing Sc during homogenization [J]. Transactions of Nonferrous Metals Society of China, 2011, 21(10): 2127−2133.
[16] XU Guo-fu, MOU Shen-zhou, YIN Zhi-ming. Effect of Sc content on the behavior of solid solution treated Al−2%Cu alloy [J]. Hunan Nonferrous Metals, 2006, 12(1): 39−40. (in Chinese)
[17] YIN Zhi-min, PAN Qing-lin, ZHANG Yong-hong, JIANG Feng. Effect of minor Sc and Zr on the microstructure and mechanical properties of Al−Mg based alloys [J]. Materials Science and Engineering A, 2000, 280(1): 151−155.

微量 Zr 和 Sc 对 Al−Mg−Si−Cu−Cr−V 合金显微组织和力学性能的影响

蒙 毅，赵志浩，崔建忠

东北大学 材料电磁过程研究教育部重点实验室，沈阳 110819

摘 要：研究微量 Zr 和 Sc 对 Al−Mg−Si−Cu−Cr−V 合金显微组织与力学性能的影响。结果表明：微量元素 Zr 和 Sc 对铸态晶粒细化、合金挤压态强度的提高以及对时效态合金中大角度晶界迁移的阻碍作用，由大到小依次为：Al_3Sc>$Al_3(Zr,Sc)$>Al_3Zr。它们均无法阻止再结晶形核，但对于时效态合金，$Al_3(Zr,Sc)$相对于位错运动的阻碍比 Al_3Sc 相更为明显。与单一添加 0.15% Sc 合金的时效态进行比较，复合添加 Zr 和 Sc 仅会轻微降低合金的强度而对塑性没有影响。综合考虑合金生产成本以及对力学性能的轻微损害等因素，在 Al−Mg−Si−Cu−Cr−V 合金中复合添加 0.13% Zr 和 0.03% Sc 是替代 0.15% Sc 的最佳方式。

关键词：Al−Mg−Si−Cu 合金；再结晶；显微组织；力学性能

(Edited by Jing-hua FANG)